

# All-band Bragg solitons and *cw* eigenmodes

A. E. Kaplan\*

*Dept. of Electrical and Computer Engineering, Johns Hopkins University, Baltimore, MD 21218*

(Dated: March 4, 2022)

We found an amazingly simple general "all-band" intensity profile of bandgap (Bragg) solitons for arbitrary parameters of spatially-periodic nonlinear systems, similar to those of multi-frequency stimulated Raman scattering, in particular the so called Lorentzian-profile solitons. We also found nonlinear eigen-modes of such system that propagate without energy exchange between waves.

PACS numbers: 42.65.-k, 42.65.Wi, 42.65.Tg, 42.81.Dp

## I. INTRODUCTION

In nonlinear optics, solitons, both temporal and spatial, became familiar objects, which can be originated by quite a few fundamental nonlinear processes. The ones of interest here are so called gap (or Bragg) solitons [1-5] (for review, see e. g. [6]) that are due to the interaction of light with spatially-periodic nonlinear structures, whereby counterpropagating waves are strongly coupled to each other *via* distributed back-and-forth Bragg reflection. The Bloch theory of *linear* periodic structures predicts the existence of "prohibited" zones – bandgaps – where due to resonances between incident wavelength and the period of spatial modulation, the incident wave cannot propagate for long, and the structure becomes almost fully reflective; those are essentially multilayered Bragg reflectors. The spectral width of such a bandgap is proportional to the contrast between refractive indices of constituent materials (or waveguide). When these refractive indexes also depend on the light intensity (e. g. due to Kerr-like nonlinearity – self-focusing if positive, self-defocusing if negative), the system may exhibit a rich host of nonlinear effects, some of the most interesting being gap solitons that emerge as a critical phenomenon, whereby the light with its frequency being inside the bandgap, "pushes" the bandgap edge away and carves conditions for itself to penetrate deep into the structure by forming gap solitons.

A new property of bandgap solitons, predicted first in [1], which gave them a distinct place amongst the soliton crowd, was that they may exist as standing (immobile, stationary) field objects. In fact, they might be viewed as a simplest, 1D-self-trapping of light. It was demonstrated then [2] that under certain conditions those solitons could be similar to familiar nonlinear solitons in regular fibers [3] and 2D-self-focusing [4] and be governed by a rescaled cubic Schrödinger equation.

In further development, it has been shown [5] that Bragg systems can support even more general gap solitons that have non-zero but very slow group velocity, giving rise to nonlinear "slow light" objects. The slow

bandgap (SBG) solitons have later been observed experimentally in [7], and immobile solitons – in [8]. Gap solitons have by now been shown to emerge in many other bandgap systems, such as e. g. in a Bose-Einstein gas [9] and near critical point in underdense plasma due to relativistic nonlinearity of electrons [10]. While SBG-solitons have been shown [5] to exist within a linear bandgap, an approximate analytical solution in [5] have been found only at a close vicinity of the bandgap edge (which in the case of self-focusing nonlinearity we call here a "blue edge", see Section IV below). Its intensity profile was again similar to nonlinear Schrödinger equation soliton. (As one can see below, Section IV, it is the weakest and longest soliton.) A greatly important development in the field was a proof [11] (based on generalization of a so called "massive Thirring model", see references in [11]) that related coupled nonlinear partial differential equations are fully integrable, which in particular allowed for a complex solution for stationary SBG-solitons with an arbitrary detuning within a bandgap.

In this paper we show that the family of intensity profiles of all the solitons within the entire Bragg bandgap are described by a simple elegant general formula (see Eqs. (3.6) and (4.1) below), which may be called an all-band Bragg soliton, derived by us based on a standard Bragg wave equation (Section II) and directly looking for a solution that satisfies the conditions of a fixed group velocity and bright-soliton asymptotic (Section III). It can be shown that these solutions are consistent with the general results [11], yet their analytical simplicity and transparency related to the use of intensities and phases as output variables, allowed for easy visualization and analysis of the soliton intensity profiles, in particular in the less studied, and perhaps the most interesting area near red-edge of the bandgap (for a positive Kerr-nonlinearity), where they assume an extremely simple yet unusual for solitons Lorentzian profile, see (4.5) below, which was missing in [11]; they are similar to a limiting case of Raman scattering solitons [12]. This approach also brings up all the relevant invariants of motion. We analyzed in detail both moving (Section IV) and stationary solitons (Section V). Using a similar approach for *cw*, *non – soliton*, solution, we found *cw – eigenmodes* of the system, in particular in a ring Bragg reflector (Section VI), and discussed the ramification and possible applications of our results (Section VII).

---

\*Electronic address: alexander.kaplan@jhu.edu

## II. WAVE PROPAGATION MODEL: BRAGG REFLECTION + KERR-LIKE NONLINEARITY

Considering a 1D-model (e.g. as in an optical fiber), we assume that the periodic grating in it is formed by the modulation of the refractive index,  $n$  (this can also be done by slight periodic tapering of fiber, which can be dealt with by a similar math-description.) In a uniform, unmodulated ( $n = \text{const}$ ) fiber the electric field  $E$  propagation is governed by a regular wave equation

$$\partial^2 E / \partial z^2 - (n^2/c^2) \partial^2 E / \partial t^2 = 0 \quad (1.1)$$

which in low-dispersion case can be decomposed into the set of two first-order equations for "forward",  $E_1$ , and "backward",  $E_2$ , traveling waves as:

$$(-1)^j \partial E_j / \partial z - (n/c) \partial E_j / \partial t = 0; \quad j = 1, 2 \quad (1.2)$$

whose  $\omega$ -monochromatic radiation solution is  $E_j = A_j \exp[-i(-1)^j k z - i\omega t]/2 + \text{c.c.}$ , with  $A_j = \text{const}$ , and  $k = \omega/cn = 2\pi/n\lambda$ ,  $n$  is an unperturbed refractive index, and  $\lambda$  is a free space wavelength. (As is common in the bandgap theory, we will neglect here the intrinsic dispersion of  $n(\omega)$  in a fiber, since the bandgap dispersion due to index modulation greatly exceeds that of a regular waveguide [5].)

A spatially modulated fiber making a periodic grating with a period  $L_B$ , has its resonant Bragg wavenumber, free space wavelength, and frequency respectively as  $k_B = \pi/L_B$ ,  $\lambda_B = 2n_0 L_B$  and  $\omega_B = k_B c/n_0$ ; a normalized half-width of a linear bandgap around  $\omega_B$  is  $\mu = \Delta n/n_0 \ll 1$ , where  $\Delta n$  is the index modulation amplitude. No radiation with  $\Delta^2 \leq \mu^2$  is allowed then to propagate in a sufficiently long system; here  $\Delta = \omega/\omega_B - 1$  is a normalized Bragg detuning. Furthermore, in the presence of a Kerr-like nonlinearity, refractive index depends on the intensity of light as  $n = n_0 + n_K E^2$ , where  $n_K$  is a coefficient due to  $\chi^{(3)}$  (Kerr) nonlinearity. The total refractive index can be written then as

$$n = n_0 + \Delta n \cos(2k_B z) + n_K E^2 \quad (1.3)$$

Generalizing (1.1) to have the index  $n$  as in (1.3), and seeking its solution as the sum of traveling waves,  $E = E_1 + E_2$ , with

$$E_j = A_j(t, z) \exp[-i\omega_B(1 + \Delta)t - i(-1)^j k_B z]/2 + \text{c.c.}; \quad (1.4)$$

with  $j = 1, 2$ , presuming the envelopes  $A_j$  to vary slowly in time and space, as  $|\Delta n|, |n_K E^2| \ll n_0$ , and neglecting higher-harmonics generation (a common approach [1-6] in nonlinear Bragg reflection because of large difference in phase velocities), we obtain truncated equations of evolution being nonlinear+modulated counterparts of (1.2) for those envelopes as:

$$i \left[ -(-1)^j \partial A_j / k_B \partial z + \partial A_j / \omega_B \partial t \right] + A_j \Delta + \mu A_{3-j} +$$

$$(n_K/n_0)(|A_j|^2 + 2|A_{3-j}|^2)A_j = 0; \quad j = 1, 2 \quad (1.5)$$

where the factor 2 in the nonlinear term is originated by intensity-induced non-reciprocity [13]. In linear case Eq. (1.5) is similar to coupled equations for counterpropagating modes in a Bragg reflector [14].

To normalize (1.5), we use the scales for intensity,  $E_{NL}^2 = \Delta n/n_K$ , distance,  $z_{NL} = 1/\mu k_B$ , and time,  $t_{NL} = 1/\mu \omega_B$ . Introducing then dimensionless envelopes,  $a_j = A_j/E_{NL}$ , time  $\tau = t/t_{NL}$ , and distance  $\zeta = z/z_{NL}$ , we rewrite (1.5) as:

$$i \left[ -(-1)^j \frac{\partial a_j}{\partial \zeta} + \frac{\partial a_j}{\partial \tau} \right] + a_j \delta + a_{3-j} +$$

$$s_K (u_j^2 + 2u_{3-j}^2) a_j = 0; \quad u_j^2 \equiv |a_j|^2 \quad (1.6)$$

where  $s_K = \text{sign}(n_K/\Delta n)$ . For a fixed  $s_K$ , only one controlling parameter, a normalized detuning  $\delta = \Delta/\mu = (\omega/\omega_B - 1)n_0/\Delta n$ , is left in (1.6). A linear band is constituted then by the condition  $\delta^2 \leq 1$ .

## III. WAVES WITH FIXED GROUP VELOCITY

As a next step let us find the solution of (1.6) for the class of modulated coupled waves with a fixed group velocity,  $\beta = \mathbf{v}_{gr} n_0/c$ , ( $\beta^2 \leq 1$ ); the solitons will be part of that family. To that end, we assume that in the frame moving with that velocity, i. e. "comoving frame", the fields are time-independent. Introducing then time-space variables in that frame as  $\zeta_\beta = \zeta - \beta\tau$ ,  $\tau_\beta = \tau$ , we are looking for the solutions with  $\partial/\partial\tau_\beta = 0$  to derive ordinary nonlinear differential equations

$$-i[\beta + (-1)^j]a'_j + \delta a_j + a_{3-j} + s_K(u_j^2 + 2u_{3-j}^2)a_j = 0 \quad (2.1)$$

where "prime" stands for  $d/d\zeta_\beta$ . To elucidate direct results for the intensity profiles, from this point, as different from [11], we will be using an "amplitude&phase" approach similar to our previous work [15,10], which greatly simplifies the calculations. To that end, we write  $a_j = u_j \exp(i\phi_j)$  with  $u_j$  and  $\phi_j$  - real, rewrite (2.1) as

$$-[\beta + (-1)^j](iu'_j - \phi'_j u_j) + u_j[\delta + s_K(u_j^2 + 2u_{3-j}^2)] + u_{3-j} e^{i(\phi_{3-j} - \phi_j)} = 0 \quad (2.2)$$

and separate real and imaginary parts in Eq. (2.2):

$$[1 + (-1)^j \beta]u'_j = u_{3-j} \sin(\phi_1 - \phi_2); \quad (2.3)$$

$$u_j [(-1)^j + \beta]\phi'_j - [\delta + s_K(u_j^2 + 2u_{3-j}^2)] = -u_{3-j} \cos(\phi_1 - \phi_2). \quad (2.4)$$

Using eq (2.3) for both  $j = 1$  and  $j = 2$ , we have  $(u_1^2 - u_2^2)' = \beta(u_1^2 + u_2^2)'$ , hence the invariant of motion for this class of solutions:

$$(u_1^2 - u_2^2) - \beta(u_1^2 + u_2^2) = D = \text{inv} \quad (2.5)$$

Using this in (2.3) and (2.4) and introducing "combined" variables

$$S = u_1^2 + u_2^2; \quad \Phi = \phi_1 - \phi_2; \quad \Sigma = \phi_1 + \phi_2; \quad P = u_1 u_2 \quad (2.6)$$

we see that their spatial dynamics is governed by equations:

$$S' = \frac{4P \sin \Phi}{1 - \beta^2}; \quad P' = \frac{S(1 - \beta^2) - \beta D}{1 - \beta^2} \sin \Phi \quad (2.7)$$

$$\Phi' = -\frac{2(\delta + s_K S) + [S(1 - \beta^2) - \beta D](s_K - \cos \Phi/P)}{1 - \beta^2} \quad (2.8)$$

$$\Sigma' = -\frac{2\beta(\delta + s_K S) - D(s_K - \cos \Phi/P)}{1 - \beta^2} \quad (2.9)$$

From eqns (2.7) we obtain phase space equation for  $P, S$  independent of  $\Phi$  and  $\Sigma$ , which greatly simplifies further calculations by separating those variables:

$$\frac{dS}{dP} = \frac{4P}{S(1 - \beta^2) - \beta D} \quad (2.10)$$

whose solution, e. g. for  $P(S)$ , is immediately found as

$$P(S) = \sqrt{(1 - \beta^2)(S - S_{min})[(S + S_{min})/2 - \beta D]/2} \quad (2.11)$$

where  $S_{min}$  is an integration constant chosen in such a way that  $P = 0$  when  $S = S_{min}$ . Having this result and using (2.8) and first eqn (2.7), we obtain now a phase space eqns for  $\Phi, S$ , as

$$d\Phi/dS = \quad (2.12)$$

$$-\frac{2(\delta + s_K S) + [S(1 - \beta^2) - \beta D][s_K - \cos \Phi/P(S)]}{4P(S) \sin \Phi}$$

#### IV. ALL-BAND MOVING SOLITONS

The solution of (2.12) in the form e. g.  $\Phi(S)$ , being substituted in (2.7) and (2.8), after integration yields  $S, P$ , and  $\Phi$  as function of  $\zeta_\beta$ . In general, all of them can be shown to be periodic functions of the distance  $\zeta_\beta$ , except for solitons. The so called bright solitons must then satisfy the condition,

$$u_j \rightarrow 0 \quad \text{at} \quad |\zeta| \rightarrow \infty \quad (3.1)$$

From (2.5) then  $D = 0$ , hence  $u_1^2 - u_2^2 = \beta(u_1^2 + u_2^2)$ . From (2.10) and (2.11) we have also that  $S_{min} = 0$  and

$$P = S\sqrt{1 - \beta^2}/2, \quad (3.2)$$

so that eqn (2.12) for variables  $S$  and  $\Phi$  reads now as:

$$\frac{d\Phi}{dS} = -\frac{2\delta + s_K S(3 - \beta^2) - 2\sqrt{1 - \beta^2} \cos \Phi}{2S \sin \Phi \sqrt{1 - \beta^2}} \quad (3.3)$$

the solution of which is readily found as  $\cos \Phi = C/S + [\delta + S(3 - \beta^2)/4]/\sqrt{1 - \beta^2}$  where  $C$  is yet another integration constant. Due to (3.1) we set  $C = 0$ , so finally

$$\cos \Phi = [\delta + s_K S(3 - \beta^2)/4]/\sqrt{1 - \beta^2} \quad (3.4)$$

Using (3.4) and (3.2) in the first eqn (2.7), we obtain a first order eqn for one variable,  $S(\zeta_\beta)$ , alone

$$S' = 2S \frac{\sqrt{1 - \beta^2} - [\delta + s_K S(3 - \beta^2)/4]^2}{1 - \beta^2} \quad (3.5)$$

whose elegantly simple yet little familiar in the soliton theory solution can be readily found:

$$S = \frac{S_{pk}(1 + B)}{\cosh[\alpha(\zeta_\beta - \zeta_0)] + B}; \quad B = \frac{\delta s_K}{\sqrt{1 - \beta^2}} \quad (3.6)$$

where combined peak intensity,  $S_{pk}$ , and size-related parameter  $\alpha$  are

$$S_{pk} = \frac{4\sqrt{1 - \beta^2}(1 - B)}{3 - \beta^2}, \quad \alpha = \frac{2\sqrt{1 - \beta^2 - \delta^2}}{1 - \beta^2} \quad (3.7)$$

In (3.6) the soliton peak position,  $\zeta_0$ , is yet another integration constant; without loss of generality we will assume  $\zeta_0 = 0$ .

Amazingly, profiles (3.6) that suggest a broad control of the shape and width of a soliton determined by parameters  $\alpha$  and  $B$  (notice here that  $B$  can be either negative or positive), coincide with the soliton profiles that show up in the multi-cascade stimulated Raman scattering [12], with completely different mechanism of their formation. Apparently, such solitons are common solutions for many situation and system with interference between waves with different wave-vectors: in those two examples either co-propagating waves (as in Raman scattering), or counter-propagating waves (as in Bragg scattering).

Individual waves intensities are now found *via* (2.5) as

$$u_1^2 = S(1 + \beta)/2; \quad u_2^2 = S(1 - \beta)/2. \quad (3.8)$$

Substituting (3.6) into (3.4), we have an expression for the phase difference  $\Phi \equiv \phi_1 - \phi_2$ :

$$\cos \Phi = \frac{1 + B \cosh(\alpha \zeta_\beta)}{B + \cosh(\alpha \zeta_\beta)}; \quad \text{or}$$

$$\tan \Phi = \frac{\sqrt{1 - \beta^2 - \delta^2} \sinh(\alpha \zeta_\beta)}{\sqrt{1 - \beta^2} [1 + B \cosh(\alpha \zeta_\beta)]} \quad (3.9)$$

At the peak,  $\zeta_\beta = 0$ , we have  $\Phi = 0$ , so the counter-propagating waves are of the same phase at that point,  $\phi_1 = \phi_2$ . At  $\zeta_\beta \rightarrow \infty$ , we have  $\tan \Phi \rightarrow \sqrt{1 - \beta^2 - \delta^2}/\delta$ .

At the exact resonance,  $\delta = 0$ ,  $\Phi$  is reversed by  $\pi$  as we go from  $\zeta_\beta = -\infty$  to  $\zeta_\beta = \infty$ . Tedious but mundane calculations show that Eqns. (3.7) – (3.9) are consistent with results [11] (see Eq. (6) in [11]); in particular, the major soliton parameter  $Q$  in [11] is related to the parameters used here *via*  $\cos Q = B$ . The simplicity and transparency of (3.7) – (3.9) however, allows one to easily analyze the soliton intensity profiles, in particular in the less studied, and perhaps the most interesting area near red-edge of the bandgap (for a positive Kerr-nonlinearity), where they assume an extremely simple yet unusual for solitons Lorentzian profile, see (4.5) below.

Notice from (3.6) – (3.8) that the bandgap for the moving solitons with a given velocity,  $\beta$ , is narrower than in the linear case:  $\delta^2 < 1 - \beta^2$ . By the same token, near both the edges of a bandgap,  $1 - \delta^2 \ll 1$ , only slow solitons are allowed, since then  $\beta^2 < 1 - \delta^2$ . On the other hand, in the middle of the bandgap,  $\delta = 0$ , the solitons are allowed with the speed up to the maximum  $\beta^2 = 1$ .

## V. STATIONARY (IMMOBILE) SOLITONS

For immobile, or stationary, solitons,  $\beta = 0$ , we have  $u_1^2 = u_2^2 = S/2$  (hence the analogy to standing waves), and the combined intensity profile,  $S$ , and phase  $\Phi$  are found from (3.6) and (3.9) as

$$S = \frac{4(1 - \delta^2)/3}{\delta + \cosh(2\zeta\sqrt{1 - \delta^2})}; \quad (4.1)$$

$$\tan \Phi = \frac{\sqrt{1 - \delta^2} \sinh(2\zeta\sqrt{1 - \delta^2})}{1 + \delta \cosh(2\zeta\sqrt{1 - \delta^2})} \quad (4.2)$$

Since this analytical solution in the entire bandgap, i. e. for any  $\delta^2 \leq 1$  is now available, one can analyze how it evolves as the laser frequency is tuned from upper (blue) edge of the bandgap,  $\delta = 1$ , to the lower (red) edge,  $\delta = -1$ . For example, close to the blue edge,  $0 < 1 - \delta \equiv \Delta\delta \ll 1$ , we have a low-intensity long pulse (see Fig. 1, lower curve):

$$S \approx \frac{4(\Delta\delta)/3}{\cosh 2(\zeta\sqrt{2\Delta\delta})}; \quad \Phi \approx \sqrt{2\Delta\delta} \tanh(\zeta\sqrt{2\Delta\delta}) \quad (4.3)$$

consistent with [5], which is a familiar soliton of a cubic Schrödinger equation, whereas at the exact Bragg resonance,  $\delta = 0$ , we have a somewhat different profile,

$$S = \frac{4/3}{\cosh(2\zeta)}; \quad \tan \Phi = \sinh(2\zeta) \quad (4.4)$$

It is worth noting that this is a solution of a generalized Schrödinger equation with the higher order nonlinearity of the 5-th order,  $\chi^{(5)}$ , whereby  $n = n_0 + n_4 E^4$  [16]. Finally, at the red edge,  $0 < 1 + \delta \ll 1$ , the main body of a standing soliton (with the maximum peak intensity) has the most unusual, Lorentzian, profile:

$$S \approx (8/3)/(1 + 4\zeta^2); \quad \tan \Phi \approx 4\zeta/(1 + 4\zeta^2) \quad (4.5)$$

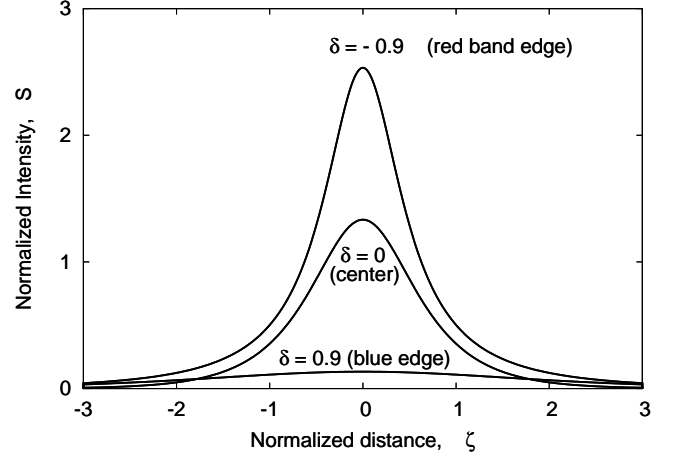


FIG. 1: Stationary solitons at various detunings  $\delta$  ( $\delta^2 < 1$ )

similar to a limiting case of stimulated Raman scattering solitons [12]. Of course, far away from the peak,  $\zeta^2 \gg (1 - \delta^2)^{-1}$ , its profile decays exponentially,  $S \propto \exp(-2\zeta\sqrt{1 - \delta^2})$ .

The total power carried by a stationary soliton in general case, i. e. for arbitrary  $\delta$ , is

$$W(\delta) = \int_{-\infty}^{\infty} S d\zeta = \frac{8}{3} \tan^{-1} \sqrt{\frac{1 - \delta}{1 + \delta}} \quad (4.6)$$

and the soliton width in the  $\zeta$ -axis at the half-peak intensity is

$$Z_{1/2}(\delta) = \frac{\cosh^{-1}(2 + \delta)}{\sqrt{1 - \delta^2}} \quad (4.7)$$

At  $\delta > 0$ ,  $\Delta\delta \equiv 1 - \delta \ll 1$  (the blue edge in case of Kerr-nonlinearity), solitons are the weakest and longest:

$$S_{pk} \approx \frac{4(\Delta\delta)}{3}; \quad W \approx \frac{4\sqrt{\Delta\delta}}{3}; \quad Z_{1/2} \approx \frac{\cosh^{-1}(1)}{\sqrt{2\Delta\delta}} \quad (4.8)$$

In the middle of linear band,  $\delta = 0$ , we have

$$S_{pk} = 4/3; \quad W = 2\pi/3; \quad Z_{1/2} = \cosh^{-1}(2) \quad (4.9)$$

The solitons at  $\delta < 0$  and  $1 + \delta \ll 1$  (red edge) are the strongest and shortest ones, albeit not by much:

$$S_{pk} \approx 8/3; \quad W \approx 4\pi/3; \quad Z_{1/2} \approx 1 \quad (4.10)$$

## VI. CW EIGENMODES OF A RING BRAGG REFLECTOR

If Bragg-reflecting structure is pumped from one end, an incident wave would decay as it propagates by transferring its energy to a reflected wave due to distributed retro-reflection [13]. As one traces both of them in the forward direction, one would see the energy of both of

them diminishing away from the incidence. However, if one pumps the structure from both ends, there could be conditions when the combined back-and-forth retro-reflection may result in both waves sustaining their energy without changes. In practical terms, such a double pumping could be best attained in a ring (Sagnac) optical waveguide resonator [17] coupled to two feeding waveguides delivering counter-propagating pumping.

Thus another objects of interest here are what we call *cw* "eigenmodes", whereby both counterpropagating wave do not change as they propagate, i. e. there is *no energy exchange* between them, similarly to the eigenmodes in  $\chi^2$  and  $\chi^3$  nonlinear wave propagation [18,19]. For Bragg reflection, those eigenmodes exist in both linear and nonlinear case and are allowed only *outside* the Bragg bandgap (which becomes intensity-dependent in nonlinear medium). A very interesting aspect of such a system is that Bragg eigenmodes should coexist with a resonant eigenmodes of a Sagnac resonator, thus creating an interesting interplay of resonant effects.

The eigen-waves propagate with a constant phase velocity, i. e. in eq (1.6) we can assume  $a_j = u_j e^{iq\zeta}$  where the amplitudes  $u_j$ , and (unknown yet) normalized perturbation of the wave number  $q$  are real constants. [Note that there is no need to assume time dependence in (5.1), since the detuning of the pumping frequency has already been taken care for by  $\Delta$  in (1.4) or  $\delta$  in (1.6).] We will be seeking then for a dispersion equation between  $q$  and  $\delta$  (which in nonlinear case should also depend on the wave intensities  $u_j^2$ ) by substituting the solution  $a_j = u_j e^{iq\zeta}$  into (1.6), and derive that equation as:

$$q = \sqrt{(\delta + 3S/2)^2 - 1} - (u_1^2 - u_2^2)/2, \quad S = u_1^2 + u_2^2 \quad (5.1)$$

In linear case,  $S \ll 1$ , we have

$$q = \sqrt{\delta^2 - 1}, \quad \text{if } \delta^2 \geq 1. \quad (5.2)$$

The ratio of the amplitudes of both waves is

$$u_j/u_{3-j} = (-1)^j \sqrt{(\delta + 3S/2)^2 - 1} - (\delta + 3S/2) \quad (5.3)$$

so that in linear case,

$$u_j/u_{3-j} = (-1)^j \sqrt{\delta^2 - 1} - \delta. \quad (5.4)$$

Both waves here have the same frequency,  $\omega = \omega_B(1 + \mu\delta)$ , but their wavenumbers are different,  $k_j = k_B[1 - (-1)^j q\mu]$ . However, in a linear case this doesn't amount to non-reciprocity, since both forward and backward waves are coupled, producing a standing-like wave in the frame that moves toward the higher intensity wave with "k-Doppler" velocity  $\mathbf{v}_{Dp} = \omega_B(k_2^{-1} - k_1^{-1})/2 \approx q\mu c/n$ . In particular, at critical points,  $\delta^2 = 1$ , we have  $q = 0$ , hence  $\mathbf{v}_{Dp} = 0$ , which indicates a regular standing wave with  $u_1^2 = u_2^2$ . In a nonlinear case, an intensity induced non-reciprocity, the same as in a regular Kerr-line nonlinearity [13] is due to the term  $u_1^2 - u_2^2$  in (5.1).

In a nonlinear case, eq (5.3) suggests a nonlinear connection between the eigen-waves amplitudes,  $u_j$ , and the

frequency detuning of a respective eigen-mode solution. Indeed, for any given set of amplitudes  $u_j$ , the respective "eigen"-detuning is:

$$\delta_{eigen} = -S[1 + (u_1 u_2)^{-1}]/2 \quad (5.5)$$

which, in a linear case,  $u_j^2 \ll 1$ , is consistent with (5.4), written as  $\delta_{eigen} = -S/(2u_1 u_2) = -(u_1/u_2 + u_2/u_1)/2$ . Notice that those eigenmodes in linear case happen only outside the Bragg bandgap (5.3); in nonlinear case they also determine the boundaries of a new, nonlinearly modified band whereby  $u_1^2 = u_2^2$  and  $S = 2u_1 u_2$ :

$$\delta_{cr} = \pm 1 - 3S/2, \quad (5.6)$$

which is red-shifted by  $3S/2$  compared to the linear one if  $n_K > 0$ , and blue-shifted if  $n_K < 0$ .

## VII. DISCUSSION

The calculations in the previous section are true not only for an infinitely long fiber, but also for a ring fiber. (A latter case, however, would involve eigen-frequencies set up by the ring length.) A ring makes an easy experimental setup for the observation of those eigenmodes by using regular external pumping fibers coupled to the ring fiber. Such a ring system and its eigenmodes (both linear and nonlinear) may present a considerable interest for applications related to Sagnac effect and ring gyro based on it, since one may expect a great enhancement of the Sagnac effect and hence of the sensitivity of a laser fiber-based gyro.

We didn't discussed here the stability of those eigenmodes in strongly nonlinear regime, which can be readily analyzed using small perturbation approach, see e. g. [20], similar to the one used in the theory of modulation instability. It is worth noting however that the Bragg nonlinear reflection is known to show optical bistability [21,1,2]; our preliminary research to be published elsewhere indicates that above some critical pumping the system is actually prone to *highly multi-stable and multi-hysteretic behavior* by forming many quasi-solitons inside a finite-length fiber and switching from a  $N$  stationary-soliton mode to a  $N \pm 1$  mode, similar to the propagation of strong light in (linearly overdense) plasma layers [10].

Furthermore, self-trapped slow or stationary solitons in a fiber may be used for the energy storage in computer applications, whereby they can be controlled to switch from a stationary state to a high-speed mode and used for operational memory or logic operations. For that purpose, it may also be of interest to use e. g. *Erbium*, *Neodimium*, or *Ytterium* doped amplifying fibers or plane waveguides [17] to get them into lasing (due to distributed retro-reflection) – and at that slow-soliton supporting – mode.

Another attractive line of further research would be to move from 1D-fibers to nonlinear 3D-photon crystals, which most likely might be instrumental in attaining slow

or stationary 3D-solitons *via* the 3D-Bragg-trapping of light and realizing sort of "stopped light bullet" that would greatly advance and transform the phenomenon of a so called "light bullet" (we are referring here to a predicted by Silberberg [22] self-sustained field object moving with the speed of light of the trapping medium, and recently observed experimentally [23]). In this respect, it is encouraging that at least a 2D-trapping in the cross-section of light beam in the form of random-phase gap solitons has been observed in photonic lattices [24].

Finally, going beyond a regular Bragg-reflection from a spatially-periodic structure, one can hypothesize that a similar phenomena of slow or stationary solitons might be expected in *any* scattering (but low-absorbing and non-linear) system, most of all – in those with *stochastic* scattering. Such a system may have a "washed-out" bandgap edges, yet the main physical factors would remain the same – distributed retro-reflection of light forming quasi-standing wave and facilitating slow-soliton formation *via* nonlinearity. Those properties put it somewhere in between Bragg-reflector and slightly-overdense plasma [10].

Same as above, this idea can be further advanced by using amplifying yet scattering media, such as doped materials. There is a reasonable possibility that a strongly-scattering nonlinear system may be able to support 3D-self-trapping and to sustain of a long-lived almost unmoving 3D-"hot-ball" reminiscent of a ball-lighting, provided there is a sufficient influx of energy from outside to support inverse population and amplification in the system.

## VIII. CONCLUSION

A general "all-band" intensity profile of slow-moving and stationary bandgap (Bragg) solitons for arbitrary parameters of of nonlinearity and spacial modulation is found to be similar to the profiles of  $2\pi$  solitons of cascade stimulated Raman scattering, including "Lorentzian" solitons. Nonlinear "no-energy exchange" eigen-modes may become a promising tool in exploration and applications of such systems.

- 
- [1] W. Chen and D. L. Mills, Phys. Rev. Lett. 58, 160 (1987); D. L. Mills and S. E. Trullinger, Phys. Rev. B 36, 947 (1987).
  - [2] J. E. Sipe and H.G. Winful, Opt. Lett. 13, 132 (1988); C.M. de Sterke and J. E. Sipe, Phys. Rev. A 38, 5149 (1988), also in Progress in Optics, **XXXIII**, 203 (1994).
  - [3] A. Hasegawa and F. D. Tappert, Appl. Phys. Lett. **23**, 142 (1973)
  - [4] V. E. Zakharov and A. B. Shabat, Sov. Phys. JETP **34**, 62 (1972).
  - [5] D. N. Christodoulides and R. I. Joseph, Phys. Rev. Lett. 62, 1746 (1989).
  - [6] C.M. de Sterke, B. J. Eggleton, and J. E. Sipe, in "Spatial Solitons", edited by S. Trillo and W. Torruellas (Springer- Verlag, Berlin, 2001); Y. S. Kivshar and G. P. Agrawal, *Optical Solitons*, Academic Press, New York (2003), ch. V.
  - [7] B. J. Eggleton, R. E. Slusher, C. M. de Sterke, P. A. Krug, and J. E. Sipe, Phys. Rev. Lett. 76, 1627 (1996); B. J. Eggleton, C. M. de Sterke, and R. E. Slusher, J. Opt. Soc. Am. B 16, 587 (1999); D. Taverner, N. G. R. Broderick, D. J. Richardson, R. I. Laming, and M. Ibsen, Opt. Lett. 23, 328 (1998); P. Millar, R. M. De La Rue, T. F. Krauss, J. S. Aitchison, N. G. R. Broderick, and D. J. Richardson, Opt. Lett. 24, 685 (1999).
  - [8] D. Mandelik, R. Morandotti, J. S. Aitchison, and Y. Silberberg, Phys. Rev. Lett. 92, 093904 (2004).
  - [9] O. Zobay, S. Pötting, P. Meystre, and E. M. Wright, Phys. Rev. A, 59, 646 (1999); B. Eiermann, Th. Anker, M. Albiez, M. Taglieber, P. Treutlein, K.-P. Marzlin, and M. K. Oberthaler Phys. Rev. Lett. 92, 230401 (2004).
  - [10] A. E. Kaplan, Optics Express, **21**, 13134 (2013).
  - [11] A. B. Aceves and S. Wabnitz, Phys. Lett. A 141, 37 (1989).
  - [12] A. E. Kaplan, Phys. Rev. Lett. **73**, 1243 (1994); A. E. Kaplan and P. L. Shkolnikov, JOSA B, **13**, 347 (1996).
  - [13] A. E. Kaplan and P. Meystre, Opt. Lett., **6**, 590 (1981), and Opt. Comm., **40**, 229 (1982).
  - [14] H. Kogelnik and C. V. Shank, J. Appl. Phys. **43**, 2327 (1972); A. Yariv, IEEE J. Quant. Electr., **QE** – **9**, 919 (1973).
  - [15] A. E. Kaplan and C. T. Law, IEEE J. Quant. Electr., **QE** – **21**, 1529 (1985).
  - [16] A. E. Kaplan, Phys. Rev. Lett. **55**, 1291 (1985).
  - [17] J. Haavisto and G. A. Pajer, Opt. Lett. **5**, 510 (1980); Hsien-kai Hsiao and K. A. Winick, Opt. Express, 15, 17783 (2007).
  - [18] A. E. Kaplan, Opt. Letts, **8**, 560 (1983) and **18**, 1223 (1993).
  - [19] S. Trillo and S. Wabnitz, Opt. Lett. **17**, 1572 (1992).
  - [20] H. G. Winful, R. Zamir, and S. F. Feldman, Appl. Phys. Lett., **58**, 1001 (1991); A. B. Aceves, C. De Angelis, and S. Wabnitz, Opt. Lett., **17**, 1566 (1992).
  - [21] H. G. Winful, J. H. Marburger, and E. Garmire, Appl. Phys. Lett., **35**, 379 (1979).
  - [22] Y. Silberberg, Opt. Lett. **15**, 1282 (1990).
  - [23] S. Minardi, F. Eilenberger, Y. V. Kartashov, A. Szameit, U. Rpke, J. Kobelke, K. Schuster, H. Bartelt, S. Nolte, L. Torner, F. Lederer, A. Tünnermann, and T. Pertsch, Phys. Rev. Lett. 105, 263901 (2010).
  - [24] G. Bartal, O. Cohen, O. Manela, M. Segev, J. W. Fleischer, R. Pezer and H. Buljan, Opt. Letts., **31**, 483 (2006).